

The Role of Water in the Oligomerization Equilibria Involving Bis(pentafluorophenyl)borinic Acid in Dichloromethane Solution

Tiziana Beringhelli, Giuseppe D'Alfonso,* Daniela Donghi, and Daniela Maggioni

Dipartimento di Chimica Inorganica, Metallorganica e Analitica, Facoltà di Farmacia, Università di Milano, Via Venezian 21, 20133 Milano, Italy

Pierluigi Mercandelli* and Angelo Sironi

Dipartimento di Chimica Strutturale e Stereochimica Inorganica, CNR-ISTM, Università di Milano, Via Venezian 21, 20133 Milano, Italy

Received July 21, 2004

The ^1H , ^{19}F , and ^{11}B NMR data indicated that in CD_2Cl_2 solution monomeric bis(pentafluorophenyl)borinic acid, $(\text{C}_6\text{F}_5)_2\text{BOH}$ ($\mathbf{1}_m$), is in equilibrium with the cyclic trimer ($\mathbf{1}_t$) observed in the solid state. The position of the association equilibrium shifted to the right on increasing the concentration, on decreasing the temperature, and on decreasing solvent polarity, in the series CD_2Cl_2 , CDCl_3 , CCl_4 , in agreement with the higher polarity of the monomer (2.38 D for $\mathbf{1}_m$ and 0.65 D for $\mathbf{1}_t$, according to PM3 computations). At temperatures lower than 210 K the ^1H and ^{19}F NMR spectra revealed the simultaneous (reversible) formation of two novel compounds, which have been formulated as the $(\text{C}_6\text{F}_5)_2\text{BOB}(\text{C}_6\text{F}_5)_2$ anhydride ($\mathbf{2}$) and the trimeric species $[(\text{C}_6\text{F}_5)_2\text{BOH}]_3\cdot\text{OH}_2$ ($\mathbf{3}$), of C_2 symmetry, with a water molecule formally inserted into a B–O(H)–B bridge of $\mathbf{1}_t$, to give a very strong $\text{BO}(\text{H})\cdots\text{HO}(\text{H})\text{B}$ hydrogen bond (δ 18.6). ^1H and ^{19}F EXSY experiments at 184 K revealed exchange between $\mathbf{3}$ and $\mathbf{1}_m$, and not $\mathbf{1}_t$. The data showed that the formation of $\mathbf{3}$, observed at temperatures where the monomer–trimer equilibrium is frozen, occurs by aggregation of monomeric units and not by cycle opening from $\mathbf{1}_t$. The stabilization of the water molecule in $\mathbf{3}$ is strong enough to promote the dehydration of $\mathbf{1}$ to give the anhydride $\mathbf{2}$; for entropic reasons, the reaction occurs only at very low temperatures and is reversed on raising the temperature. At higher temperatures, the position of the monomer–trimer equilibrium is affected by the amount of water, which stabilizes the trimeric form, owing to the formation of a hydrogen-bond adduct $\mathbf{4}$ containing exocyclic water. At low temperatures, in the presence of the monomer, this species progressively dehydrated, due to the formation of $\mathbf{3}$. The amount of water present in solution also affected the rate of attainment of the $\mathbf{1}_m/\mathbf{1}_t$ equilibrium, the oligomerization being exceedingly slow in anhydrous conditions. The catalytic role of water can be attributed to the increased nucleophilicity of the BOH group upon water coordination, which allows alternative aggregation pathways. Semiempirical computations, at the PM3 level, provided a picture of the oligomerization in the presence and in the absence of water that well agrees with the experimental findings.

Introduction

We are currently investigating the association equilibria involving Lewis acids such as perfluoroarylboranes. It has been previously reported^{1,2} that tris(pentafluorophenyl)borane in toluene solution is able to bind quantitatively and in a stepwise manner up to three water molecules, the first one through a Lewis acid–base $(\text{C}_6\text{F}_5)_3\text{B}-\text{OH}_2$ interaction and the other two

via strong $\text{BO}(\text{H})\text{H}\cdots\text{OH}_2$ hydrogen bonds. More recently we have shown that bis(pentafluorophenyl)borinic acid ($\mathbf{1}$)³ in the solid state exists as a self-associated trimeric species, which in toluene solution dissociates to give the $(\text{C}_6\text{F}_5)_2\text{BOH}$ monomer (hereafter Ar_2BOH , $\text{Ar} = \text{C}_6\text{F}_5$).⁴ This molecule, owing to presence of a variety of reactive sites (Lewis acid and Lewis base, Brønsted acid, hydrogen-bond donor and acceptors) can be involved in a multiplicity of intra- or intermolecular interactions and association equilibria. An in-depth investigation of the forms in which the molecule is really present in solution is then crucial, in the light of the high current interest, both academic and industrial, for

(1) Beringhelli, T.; Maggioni, D.; D'Alfonso, G. *Organometallics* **2001**, *20*, 4927.

(2) (a) Bergquist, C.; Bridgewater, B. M.; Harlan, C. J.; Norton, J. R.; Friesner, R. A.; Parkin, G. *J. Am. Chem. Soc.* **2000**, *122*, 10581. (b) Doerrer, L. H.; Green, M. L. H. *J. Chem. Soc., Dalton Trans.* **1999**, 4325. (c) Danopoulos, A. A.; Galsworthy, J. R.; Green, M. L. H.; Cafferkey, S.; Doerrer, L. H.; Hursthouse, M. B. *Chem. Commun.* **1998**, 2529. (d) Siedle, A. R.; Lamanna, W. M. U.S. Patent 5,296,433, 1994. (e) Siedle, A. R.; Lamanna, W. M.; Newmark, R. A. *Macromol. Symp.* **1993**, *66*, 215.

(3) Chambers, R. D.; Chivers, T. *J. Chem. Soc.* **1965**, 3933.

(4) Beringhelli, T.; D'Alfonso, G.; Donghi, D.; Maggioni, D.; Mercandelli, P.; Sironi, A. *Organometallics* **2003**, *22*, 1588.

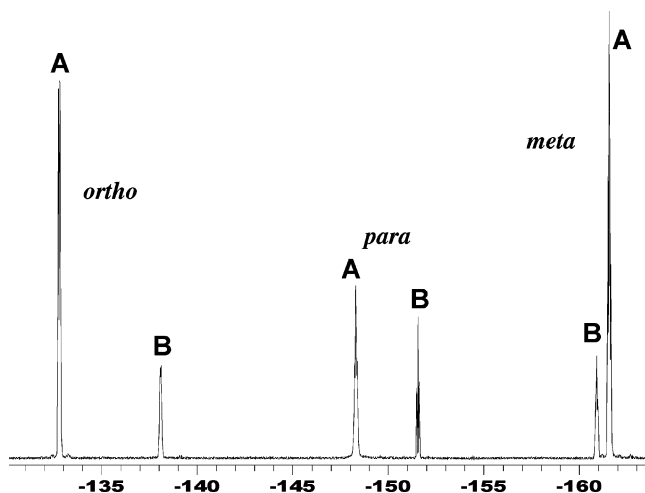


Figure 1. Typical ^{19}F NMR spectrum of a CD_2Cl_2 solution of **1** (283 K, 0.18 M). Signals **A** are due to $\mathbf{1}_m$ and **B** to $\mathbf{1}_t$.

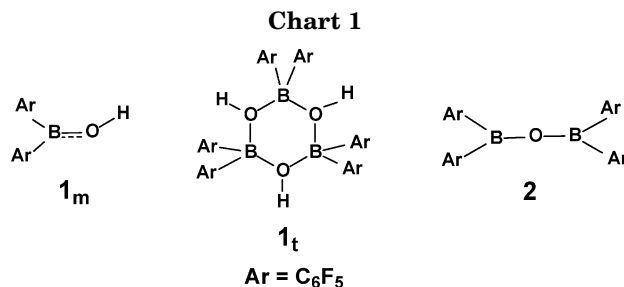
this compound.^{5,6} In particular, it has been recently shown that, in combination with aluminum alkyls, it is an efficient cocatalyst for olefin polymerization.⁷

We have already shown that the $p\pi-p\pi$ O \rightarrow B donation imparts a partial double-bond character to the B–OH interaction, responsible for the restricted rotation observed by low-temperature NMR in toluene solution.⁴

We have now investigated the behavior of **1** in dichloromethane and found a much more complex picture than in toluene. In this solvent sizable amounts of the trimeric form of Ar_2BOH are present, even at room temperature. Adventitious water, which acts as a Lewis base and as hydrogen-bond acceptor/donor, affects both the position and the rate of the monomer–trimer equilibrium, owing to the formation of a number of monomeric or oligomeric adducts. The nature of these adducts and their interconversion pathways have been investigated, also with the use of semiempirical computations. In this context, a quite unusual spontaneous dehydration reaction has been discovered, driven by the formation of a very strong hydrogen bond within an oligomeric adduct containing “endo-cyclic” water.

Results and Discussion

Monomer–Trimer Equilibrium. The ^1H and ^{19}F spectra of bis(pentafluorophenyl)borinic acid (**1**) in CD_2Cl_2 solution usually show two sets of resonances, labeled as **A** and **B** in Figure 1. The major set **A** is immediately attributed to the monomeric form ($\mathbf{1}_m$) of Ar_2BOH , on the basis of the chemical shift values (Table



1) quite close to those measured in toluene solution. The attribution of the minor set **B** to the trimeric cyclic form $\mathbf{1}_t$ (Chart 1) is based on the points below.

(i) The ^{11}B chemical shift value (δ 8.4) is typical of tetracoordinated boron atoms (while that of $\mathbf{1}_m$ falls in the range of tricoordinated boron derivatives, δ 43.8).^{8,9} (ii) The values of the longitudinal relaxation times T_1 , much shorter for resonances **B** than **A** (Table 1), indicate that the species responsible for set **B** is a molecule larger than that responsible for signals **A**. (iii) The relative intensity R of signals **B** with respect to **A** is higher in spectra recorded immediately after dissolution of **1** (in solid **1** exists in the trimeric form),⁴ then slowly decreases to equilibrium values. (iv) The equilibrium values of R increase on increasing the overall concentration (Figure 2a) and (v) on decreasing the temperature (Figure 2b).

The latter behavior is typical of association processes, which are entropically unfavorable. All of the above evidence indicates that in the present case this process is a self-oligomerization reaction.¹⁰ The occurrence of such processes is a well-known phenomenon for R_2BY derivatives in which Y contains one or more lone pairs (Y = halogens, OR, NR_2).^{9g,11} The trimeric nature of the $[\text{Ar}_2\text{BOH}]_n$ oligomer has been ascertained by measuring the slope of a suitable plot of the intensity ratios R at different overall concentrations C (as detailed in the Supporting Information, Figure S1).

It has been therefore definitely confirmed that signals **B** are due to the cyclic trimer $\mathbf{1}_t$, in equilibrium with the monomer $\mathbf{1}_m$ (eq 1). According to the NMR data (one protonic resonance, one set only of ^{19}F signals), in solution $\mathbf{1}_t$ has a (dynamic) symmetry higher than that observed in the solid state (C_2).⁴



Equilibrium 1 is slow, and its rate is affected by the presence of traces of water (as will be discussed in the

(8) Kidd, R. J. In *NMR of Newly Accessible Nuclei*; Laszlo, P., Ed.; Academic Press: New York, 1983; Vol. 2.

(9) See for instance: (a) Dagorne, S.; Guzei, I. A.; Coles, M. P.; Jordan, R. F. *J. Am. Chem. Soc.* **2000**, *122*, 274. (b) Fraenk, W.; Klapötke, T. M.; Krumm B.; Mayer, P. *Chem. Commun.* **2000**, 667. (c) Kehr, G.; Fröhlich, R.; Wibbeling, B.; Erker, G. *Chem. Eur. J.* **2000**, *6*, 258. (d) Jacobsen, H.; Berke, H.; Döring, S.; Kehr, G.; Erker, G.; Fröhlich, R.; Meyer, O. *Organometallics* **1999**, *18*, 1724. (e) Vagedes, D.; Fröhlich, R.; Erker, G. *Angew. Chem., Int. Ed.* **1999**, *38*, 3362. (f) Parks, D. J.; Piers, W. E.; Parvez, M.; Atencio, R.; Zaworotko, M. J. *Organometallics* **1998**, *17*, 1369. (g) Parks, D. J.; Piers, W. E.; Yap G. P. A., *Organometallics* **1998**, *17*, 5492. (h) Sun, Y.; Piers, W. E.; Rettig, J. R. *Organometallics* **1996**, *15*, 4110.

(10) The hypothesis that the observed association equilibrium consisted in the formation of adducts with adventitious Lewis bases (such as water) was immediately ruled out, due to the points i–iv and to the fact that signals **B** are observed even in strictly anhydrous conditions (see below).

(11) (a) Fraenk, W.; Klapötke, T. M.; Krumm B.; Mayer, P. *Chem. Commun.* **2000**, 667. (b) Parks, D. J.; Spence, R. E. von H.; Piers, W. E. *Angew. Chem., Int. Ed. Engl.* **1995**, *34*, 809.

(5) (a) Ishihara, K.; Yamamoto, H. *Eur. J. Org. Chem.* **1999**, 527. (b) Ishihara, K.; Kurihara, H.; Yamamoto, H. *J. Org. Chem.* **1997**, *62*, 5664. (c) Ishihara, K.; Kurihara, H.; Yamamoto, H. *Synlett* **1997**, 597.

(6) Recent patents dealing with synthesis or uses of **1** are: (a) Ikeno, I.; Mitsui, H.; Iida, T.; Moriguchi, T. (Nippon Shokubai Co) Patent WO 0248156, 2002. (b) Ikeno, I.; Mitsui, H.; Iida, T.; Moriguchi, T. (Nippon Shokubai Co) Patent WO 0244185, 2002. (c) Schottek, J.; Fritze, C. (Targor) Patent DE 10009714, 2001. (d) Kratzer, R. (Basell Polyolefins) Patent DE 10059717, 2001. (e) Kratzer, R.; Fritze, C.; Schottek, J. (Targor) Patent DE 19962814, 2001. (f) Frances, J. M.; Deforth, T. (Rhodia Chimie) Patent WO 0130903, 2001. (g) Schottek, J.; Fritze, C.; Bohnen, H.; Becker, P. (Targor) WO 0020466, 2000. (h) Bohnen, H.; Hahn, U. (Aventis R&T GMBH) Patent DE 19843055, 2000. (i) Bohnen, H. (Hoechst A.-G.) Patent DE 19733017, 1999.

(7) (a) Kratzer, R. (Basell Polyolefins) Patent WO 04041871, 2004. (b) Kratzer, R. (Basell Polyolefins) Patent WO 04007570, 2004. (c) Kratzer, R.; Fraaije, V. (Basell Polyolefins) Patent WO 04007569, 2004.

Table 1. ^1H and ^{19}F NMR Data (δ and T_1) for Compounds 1–3

compound ^a	T (K)	δ ^{19}F <i>ortho</i> [T_1] ^b	δ ^{19}F <i>para</i> [T_1] ^b	δ ^{19}F <i>meta</i> [T_1] ^b	δ ^1H [T_1] ^b
1_m (A)	283	-132.78 [1.95]	-148.28 [1.89]	-160.70 [2.62]	7.41 [1.6]
1_t (B)	283	-138.27 [0.36]	-151.24 [0.44]	-161.56 [0.57]	7.78 [0.5]
2 (C)	283	-132.12 [0.55]	-145.99 [0.55]	-161.14 [0.55]	
3 (D)	184	-132.5(1) ^d	-151.5(1)	-161.2(4) ^d	5.62(2) ^c
		-133.2(1)	-152.0(1)	-162.2(1)	8.07(2) ^c
		-138.3(1)	-153.0(1)		18.6(1) ^c
		-139.9(1)			
		-141.9(1)			

^a In parentheses the label used in the text to indicate each set of resonances. ^b Longitudinal relaxation times T_1 (s) measured at 253 K. ^c Attribution of the protonic signals, according to the labels of Chart 2: H_a 18.6, H_b 5.62, H_c 8.07. ^d The *ortho* and *meta* ^{19}F resonances here reported have been attributed on the basis of NOE and exchange cross-peaks in a ^{19}F - ^{19}F EXSY/NOESY experiment and of the integrated intensities. One *ortho* and one *meta* signal have not been identified with certainty.

following). In strictly anhydrous conditions, many hours are required to attain the equilibrium even at a relatively high temperature such as 283 K (see Figure S2 in the Supporting Information). From the equilibrium values measured at different temperatures in the experiment of Figure 2b, a good van't Hoff plot (shown in Figure S3, Supporting Information) was obtained. Unfortunately, these experimental equilibrium values are slightly biased toward **1_t**, due to the presence of traces of water. Therefore, the thermodynamic values estimated from the van't Hoff plot ($\Delta H^\circ = -69 \text{ kJ mol}^{-1}$, $\Delta S^\circ = -228 \text{ J K}^{-1}$) do not correspond to the true thermodynamic parameters of equilibrium 1, whose determination was hampered by the sluggishness of the equilibrium under anhydrous conditions.

Solvent Effect on the Oligomerization Equilibrium. As mentioned in the Introduction, in toluene solution, versus CD_2Cl_2 , the concentration of the trimer **1_t** is below detection limits, even at low temperatures. The reasons for the different position of equilibrium 1 on varying the solvent are not obvious.

The different polarity should act in the opposite way, because **1_t** has a lower polarity than **1_m**: B3LYP/6-31G(d,p)//PM3 computations provided a value of 2.48 D for the monomer (C_1) and 0.75 D for the trimer (C_2). In agreement with this, we have found that in the homologous series CH_2Cl_2 , CHCl_3 , CCl_4 , the equilibrium concentration of the trimer increases on decreasing solvent polarity, according to the good linear free-energy correlation shown in Figure 3 ($K = 3.9, 10.2, 44.5$, respectively, at 283 K, on passing from CH_2Cl_2 to CHCl_3 to CCl_4 , with $E_T(30)^{12} = 40.7, 39.1, 32.4$, respectively).

We suppose that the stabilization of **1_m** in toluene, despite the low polarity of this solvent, may be attributed to preferential solvation of **1_m** with respect to **1_t**, due to B–OH...arene interactions or to the higher availability of its aryl rings for interacting with the solvent aromatic rings.

Variable-Temperature Behavior: Spontaneous Partial Dehydration. On lowering the temperature, the ^{19}F spectra revealed three main changes (Figure 4). The first consists of splitting each of the signals of **1_m** into two separate resonances of equal intensity, as previously observed in toluene solution.⁴ This arises from the freezing of the hindered rotation around the B–OH bond, due to the partial double-bond character

(12) $E_T(30)$ is an empirical parameter of solvent polarity derived from the wavelength of an intramolecular charge transfer band of a suitable standard: Reichardt, C. *Angew. Chem., Int. Ed. Engl.* **1979**, *18*, 98.

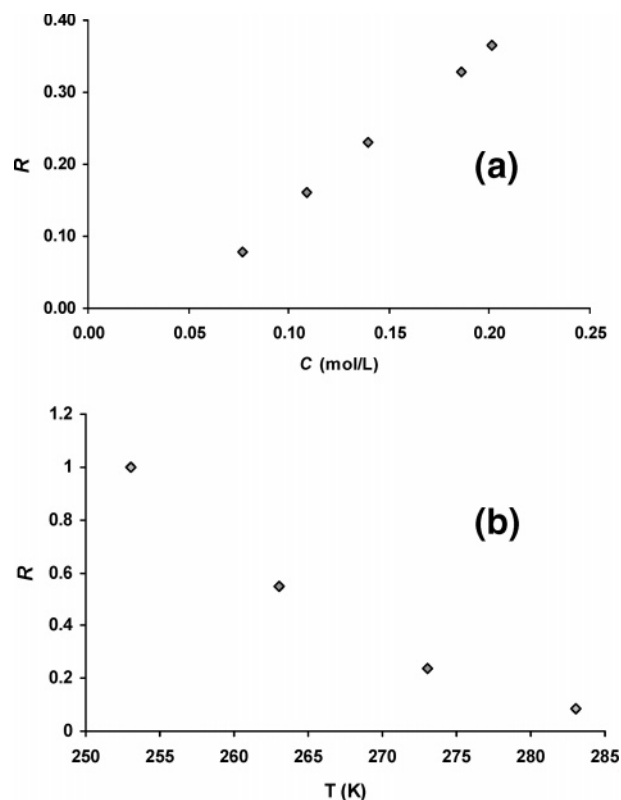


Figure 2. Variation of the relative intensity of the signals of **1_t** with respect to those of **1_m** (R , equilibrium values) on varying (a) the overall concentration of **1** (at 278 K) and (b) the temperature (in a 0.071 M solution).

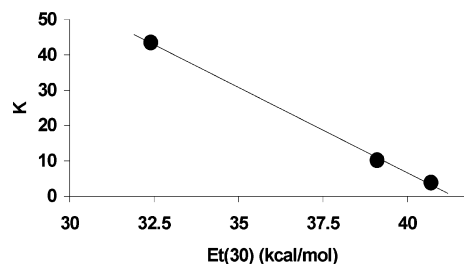


Figure 3. Plot of the constant of equilibrium **1** versus the polarity parameter $E_T(30)$ of the solvent.

of the B–O interaction,⁴ which removes the dynamic equivalence of the two aryl rings of **1_m**. Band shape analysis provided the kinetic parameters for the rotation around the B–O bond, which are identical to those estimated in toluene solution: $\Delta H^\ddagger = 41.8(5) \text{ kJ mol}^{-1}$ (vs $42.3(3)$ in toluene), $\Delta S^\ddagger = 14(3) \text{ J K}^{-1} \text{ mol}^{-1}$ (vs $13(2)$ in toluene), in agreement with the intramolecular nature of the process.

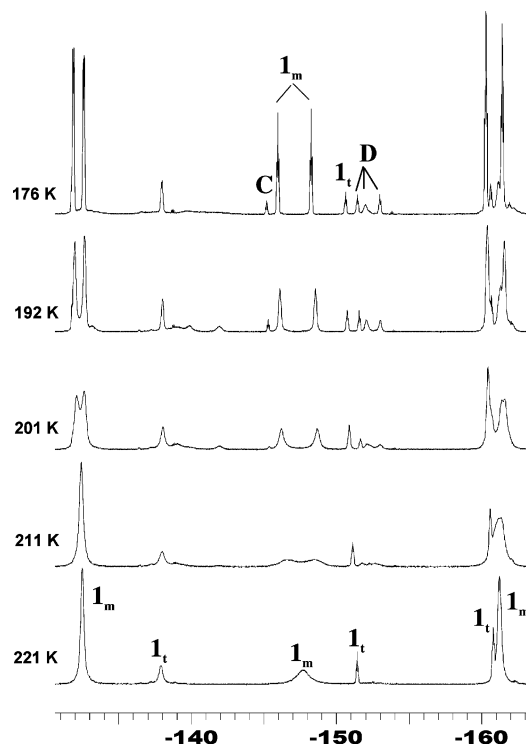
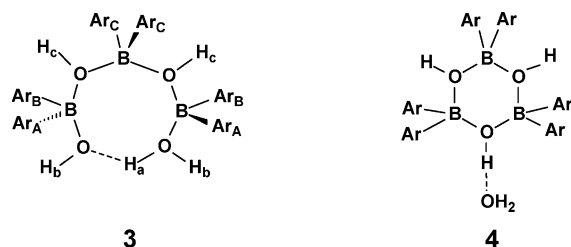


Figure 4. Variable-temperature ^{19}F spectra of a solution of **1** in CD_2Cl_2 (0.14 M).

Chart 2



The other two changes observed in the ^{19}F spectra consist of the appearance, at temperatures lower than 210 K, of two new sets of resonances, labeled with **C** and **D** in Figure 4 and Table 1. Even if their intensities were always small (and somewhat variable in different experiments), such signals are important, because they give a hint of the complex equilibria in which the title compound is involved in dichloromethane solution. The appearance of resonances **C** and **D** was perfectly reversible, and they always disappeared on increasing the temperature.

Signals **C** (for which no protonic counterpart could be identified) are attributable to the $\text{Ar}_2\text{BOBAR}_2$ anhydride (**2**, $\text{Ar} = \text{C}_6\text{F}_5$, Chart 1).^{13–15} Indeed these signals appeared, even at room temperature, when we treated dichloromethane or toluene solutions of **1** with powerful water scavengers, such as $\text{B}(\text{C}_6\text{F}_5)_3$ or P_4O_{10} , able to drive to the right equilibrium **2**. Moreover, the addition

(13) The synthesis of **2**, by reaction of **1** with $\text{ClB}(\text{C}_6\text{F}_5)_2$, and its NMR data are reported in ref 14. ^{19}F (toluene- d_6): -132.6 , -144.3 , -160.2 ppm. A recent patent⁶⁸ gives the following values (C_6D_6 solution): -134 , -146 , -161 ppm.

(14) Tian, J.; Wang, S.; Feng, Y.; Li, J.; Collins, S. *J. Mol. Catal. A: Chem.* **1999**, *144*, 137.

(15) The structure of **2** has been determined by X-ray crystallography, and some metrical parameters are cited in: Piers, W. E.; Irvine, G. J.; Williams, V. C. *Eur. J. Inorg. Chem.* **2000**, 2131.

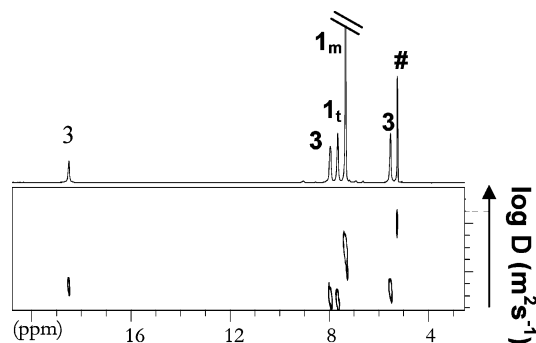


Figure 5. ^1H DOSY spectrum of a CD_2Cl_2 solution of **1** ($\# = \text{solvent}$, 0.16 M, 170 K, 11.7 T).

of even small amounts of water to these solutions caused the instantaneous disappearance of these signals, with a corresponding increase of the signals of $\mathbf{1}_m$.



In the absence of external water scavengers, the driving force for dehydration of **1** is the formation at low temperature of the species responsible for resonances **D**. Such species has been formulated as the adduct $[(\text{Ar}_2\text{BOH})_3 \cdot \text{H}_2\text{O}]$ (**3**) depicted in Chart 2, on the basis of the experimental information summarized below.

The presence of three separate *para* signals indicates that **3** contains three Ar_2BOH units.¹⁶ The oligomeric nature of this species has been confirmed by a ^1H DOSY experiment (performed at 170 K), which showed that the diffusion coefficient of **3** was very similar to that of $\mathbf{1}_t$ (Figure 5). The ^1H spectrum of **3** (three signals, in the ratio 1:2:2, Table 1) suggested the presence of one water molecule. In agreement with this, the addition of $\text{B}(\text{C}_6\text{F}_5)_3$ as water scavenger caused the instantaneous and complete disappearance of the signals of **3**, while a (small) addition of water at low temperature (see below) increased their relative intensity. The 1:2:2 pattern of the protonic resonances implies (true or dynamically generated) equivalence of two Ar_2BOH units, i.e., C_2 symmetry. The very low-field resonance of the singular proton (δ 18.6) indicates that it is involved in a strong hydrogen bond.

Structure and Dynamics of 3. The above evidence would agree with both structures **3** and **4** of Chart 2. However 2D ^{19}F (Figure 6) and ^1H (Figure 7) EXSY experiments at 184 K showed exchange cross-peaks between the resonances of **3** and those of $\mathbf{1}_m$, while negligible exchange cross-peaks were observed with $\mathbf{1}_t$ at all the temperatures where species **3** was detectable. This ruled out structure **4**: indeed, if water was simply H-bonded to the trimer, exchange with $\mathbf{1}_t$ and not with $\mathbf{1}_m$ should occur. Therefore in **3** the ring closure necessary to account for the C_2 symmetry occurs via a hydrogen-bond interaction between a proton of coordinated water and the oxygen of the Ar_2BOH unit at the opposite end of the trimeric chain. This hydrogen bond, even if very strong (δ 18.6), is labile enough to allow exchange of the terminal Ar_2BOH unit with free $\mathbf{1}_m$.

(16) The related *ortho* and *meta* signals are hardly detectable (Figure S5 in Supporting Information), since they are broadened for the slowing of the hindered rotation around the boron–carbon bonds, and some of them are also buried under the stronger $\mathbf{1}_m$ and $\mathbf{1}_t$ resonances.

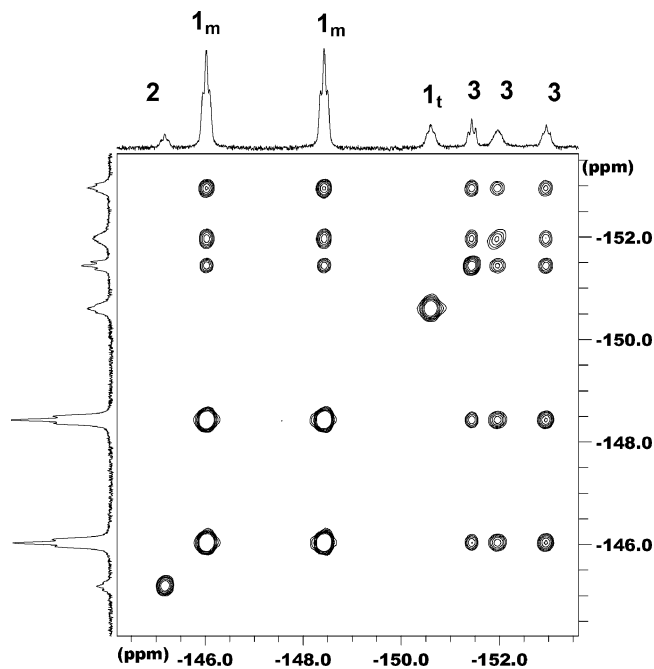


Figure 6. 2D ^{19}F EXSY (region of the *para* fluorine atoms) of a 0.076 M CD_2Cl_2 solution of **1** at 184 K.

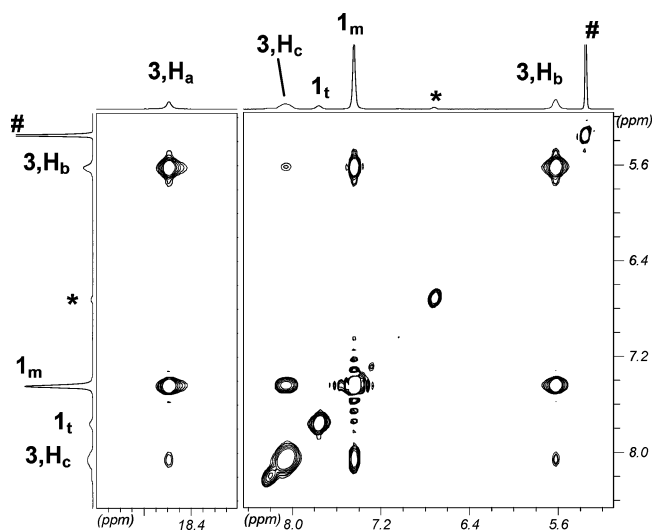


Figure 7. 2D ^1H EXSY spectrum of **1** (184 K, CD_2Cl_2 (#), 0.12 M). The asterisk marks an unidentified impurity.

There is evidence that this $\text{B}(\text{H})\text{O}\cdots\text{H}_a\cdots\text{O}(\text{H})\text{B}$ hydrogen bond is not symmetrical (Chart 2); that is, the C_2 symmetry is not true, but dynamically generated. Indeed at the lowest temperatures the ^1H signal due to H_b broadened and decoalesced into two very broad separated resonances (as shown in Figure S4 of the Supporting Information).¹⁷ Therefore, the observed C_2 symmetry results from rapid proton migration between the two oxygen atoms. This rapid oscillation makes in turn each of the two involved Ar_2BOH groups a chain terminal (if the H-bond is ignored), ready to exchange with free **1_m**. This mechanism implies that the aryl groups Ar_A and Ar_B of Chart 2 should have a higher exchange rate with **1_m** than those of the “inner” Ar_2BOH moiety (Ar_C). In agreement with this, Figure 6 shows

(17) Broadening and collapse was observed also in the *para* ^{19}F region, even if in this case the conditions for decoalescence were not achieved.

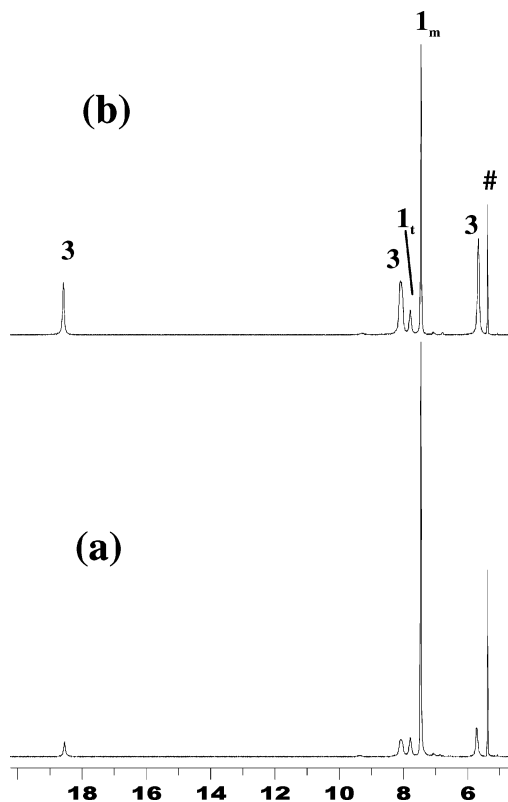


Figure 8. ^1H NMR spectra at 178 K of (a) a 0.10 M solution of **1** in wet CD_2Cl_2 (#); (b) the same, after the addition of 0.1 μL of water at 193 K.

that the lowest field *para* resonance of **3** has cross-peaks with **1_m** weaker than those (of equal volumes) of the other two resonances. This signal is then attributed to Ar_C . Fast rotation of the water molecule around the B–O bond accounts for the observed exchange between proton H_a (δ 18.6) and proton H_b (δ 5.8) (Figure 7). The exchange of both these protons with H_c was slower and possibly mediated by the exchange with **1_m** (which in turn exchanges faster with H_a and H_b than with the “inner” protons H_c , Figure 7).

A $\{^{19}\text{F}\}^1\text{H}$ experiment at 173 K showed that the large bandwidth of the ^1H signal of the two equivalent protons H_c of **3** (δ 8.05) is due to coupling with ^{19}F : this suggests the presence of $\text{BO}-\text{H}_c\cdots\text{F}-\text{C}_{\text{aryl}}$ hydrogen bonds involving *ortho* fluorine atoms of adjacent C_6F_5 rings, as observed in the solid state structure of **1_t**.

Interaction of **1 with Water.** If dehydration of **1_m** was the only source of water present in **3**, the anhydride **2** and the water adduct **3** should form in a 1:1 ratio. In fact, the signals of **3** were always slightly more intense than those of **2** (even if the ratio between **2** and **3** was somewhat variable in different experiments). This can be attributed to the unavoidable presence of adventitious water. Indeed, the addition of water (at 193 K) strongly increased the amount of **3**, as depicted in Figure 8 for ^1H and in Figure S5 of the Supporting Information for ^{19}F . These figures show also that the formation of **3** was accompanied by the decrease of the concentration of **1_m**, while the concentration of **1_t** remained unchanged: this clearly indicated that **3** was formed at the expenses of **1_m** (eq 3).



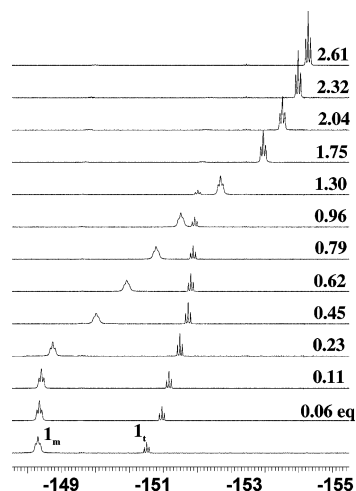
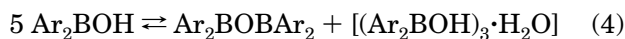


Figure 9. ^{19}F NMR monitoring of a titration with water of a CD_2Cl_2 solution of **1** (0.18 M) at 283 K (only the region of the *para* fluorine atoms is shown, for the sake of clarity). The figures on the right indicate the equivalents of added water at each titration step.

Moreover, the simultaneous formation of the anhydride **2** and of **3** can be depicted with the overall equilibrium **4**, taking into account that the trimer–monomer interconversion is frozen (even in the presence of water) at temperatures where such reaction is observed. The position of this equilibrium shifts to the right only at temperatures low enough to make less important the very unfavorable entropic term. This explains the reversibility of the formation of **3** and **2** on varying the temperature.



Further information on the interaction of **1** with water was provided by a titration performed directly into a NMR tube, at 283 K, monitored by ^{19}F (Figure 9), ^{11}B , and ^1H NMR. The scenario appearing from these data is as follows.¹⁸

(i) Water addition did not cause the appearance of novel signals,¹⁹ but rather a strong shift of the resonances of **1_m** and **1_t**. This implies that **1_m** and **1_t** are in fast exchange with their respective water adducts, so that molar fraction weighted averaged resonances are observed.

(ii) At the very beginning of the titration (up to ca. 0.3 equiv of water) the ^{19}F δ shift was stronger for **1_t** than for **1_m**. This indicates that water, when present in low concentration, interacts preferentially with **1_t**, resulting in the shift of equilibrium **1** toward the trimeric form. Indeed, the relative amount of the trimer

(18) The same behavior was observed in an analogous titration experiment at lower temperature (253 K). At both temperatures, the ^1H NMR monitoring provided poor information, since the addition of even very small amounts of water produced one broad averaged resonance, which progressively sharpened on further increasing the amount of water (see Figure S6): the comparison of the ^1H and ^{19}F data shows that water promotes proton exchange processes, whose rate increases with water content. This hampered the identification of the resonances of the water molecules interacting with borinic acid.

(19) The only novel species observed was pentafluorobenzene, formed in very low concentration from the transformation of some **1** into $(\text{C}_6\text{F}_5)\text{B}(\text{OH})_2$ and then into $\text{B}(\text{OH})_3$. This reaction is known to slowly occur in the presence of water (Bradley, D. C.; Harding, I. S.; Keefe, A. D.; Montevalli, M.; Zheng, D. H. *J. Chem. Soc., Dalton Trans.* **1996**, 3931). The ^{19}F signals of the boronic acid are not observed due to its poor solubility.

slightly but significantly increased at the initial titration stages (see Figure 10a). The interaction of water with **1_t** most likely occurs through H-bonding, to give adduct **4** of Chart 2, rather than species **3**. Indeed the formation of the latter species is expected to shift the signals of **1_m** rather than those of **1_t**, since at these temperatures its exchange with **1_m** (detectable even at 173 K) should be so fast to dynamically average their signals.²⁰

(iii) The stabilization of the trimeric form resulting from its interaction with water was not strong enough to allow the complete transformation of the monomer into the trimer (at least at 283 K). Then, on continuing with the titration, the initial trend was reversed: the relative intensity of the signals of the trimeric species (**1_t** plus **4**) progressively decreased, and strong (upfield) shifts were shown by the ^{19}F and ^{11}B signals of **1_m** (Figures 9 and 10). Therefore at this point of the titration added water was captured mainly by **1_m**, so that its adduct/adducts with water became the dominant species.²¹ Above 2 equiv the concentration of trimeric species was negligible.

The plots of Figures 10b–d suggest that **1_m** may be able to bind up to two water molecules. As to the nature of these adducts, the ^{11}B spectra showed that, as soon as water uptake by **1_m** became significant, the ^{11}B signal of the monomer began shifting from the region of trito that of tetracoordination (Figure 10d). Therefore **1_m** binds water through a covalent $\text{Ar}_2(\text{OH})\text{B}-\text{OH}_2$ Lewis acid–base bond, rather than a hydrogen-bond interaction, to give the adduct **5** of Scheme 1.²² Most likely, the hydrogen bond is responsible for the binding of the second water molecule, as shown in Scheme 1.²³

Role of Water in the Oligomerization Equilibrium. The titration experiments have shown that the amount of water present in solution affects the posi-

(20) The ^1H NMR spectra provided another piece of evidence supporting the idea that the traces of water are preferentially H-bonded to **1_t**. Even if the ^1H spectra (283–253 K) are useless at relatively high water content (due to the presence of broad averaged resonances),¹⁸ separated resonances for trimeric and monomeric species can be observed when water content is really low. In these cases the change of their δ on varying the amount of water was significantly different (see for instance Figure S6): the signal of the trimer shifted to higher frequency, as expected for the increase of the fraction of **1_t** involved in hydrogen-bonding interaction. By contrast, the signal of the monomer became very broad and shifted to higher field. The latter behavior, observed even in the absence of significant **1_m**· H_2O adduct formation (as revealed in the case of Figure S6, step b, by the comparison with the corresponding ^{19}F spectrum), must be attributed to fast proton exchange with the water molecules (mostly H-bonded to **1_t**, but in minor amount covalently bonded to **1_m** or even free). Noteworthy, it has been impossible to identify the resonances of water interacting with either **1_m** or **1_t**, most likely due to such easy exchange. The comparison of the ^1H and ^{19}F integration ratios between **1_m** and **1_t** supports the idea that the protonic signal of **1_m** incorporated the water signal. The addition of molecular sieves directly into the NMR tube reversed the effects of water addition: the signal of the trimer shifted back to higher field, and that of the monomer sharpened.

(21) According to a (probably oversimplified) model involving equilibrium **1** (K_1) and the equilibria of water uptake by **1_t** (K_2) and **1_m** (K_3), the ratio between trimeric (**1_t**+**4**) and monomeric (**1_m** plus its water adduct) species should be proportional to $[\text{1}_m]^2(1 + K_2[\text{H}_2\text{O}]) / (1 + K_3[\text{H}_2\text{O}])$, the proportionality constant being (K_1K_2/K_3) . In the course of the titration, the fractional term containing $[\text{H}_2\text{O}]$ slightly increases (if **1** was not negligible with respect to $K_1[\text{H}_2\text{O}]$ and $K_2 > K_3$), but $[\text{1}_m]$ decreases, and eventually the latter effect becomes dominant, making progressively smaller the concentration of the trimeric species.

(22) The concentration of **3** (and of the other oligomeric species arising from the association equilibria involving **5** discussed below and depicted in Scheme 2) is negligible at a temperature as high as 283 K. Moreover, the importance of these oligomerization equilibria is obviously progressively reduced as the increase of the amount of water reduces the concentration of free **1_m**.

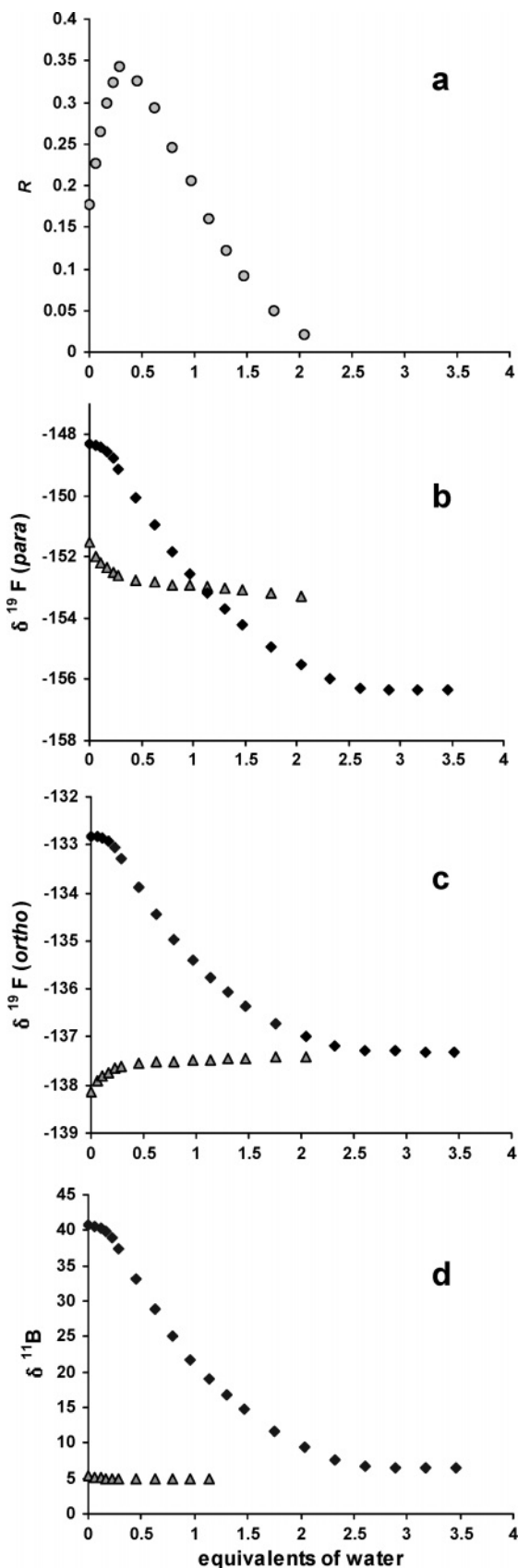
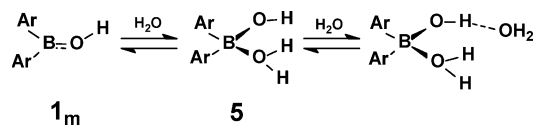


Figure 10. Titration of **1** with water, at 283 K: (a) change of the relative intensity of the ^{19}F signals of $\mathbf{1}_t$ with respect to those of $\mathbf{1}_m$ (R) in the titration course; (b–d) simultaneous variation of the chemical shifts of the ^{19}F *para* (b), ^{19}F *ortho* (c), and ^{11}B resonances (d) of the monomeric (\blacklozenge) and of the trimeric species (\blacktriangle) (averaged signals for $\mathbf{1}_m$ and its water adducts, and for $\mathbf{1}_t$ and its water adducts).

Scheme 1. Stepwise Addition of Water on $\mathbf{1}_m$



tion²⁴ and the bandwidth²⁵ of the signals (since they become molar fraction weighted averaged resonances) and also modifies the position of the $\mathbf{1}_m \rightleftharpoons \mathbf{1}_t$ equilibrium. As mentioned above, the determination of the true values of the constants of this equilibrium has been hampered by the extreme slowness of the monomer–trimer interconversion in the absence of water.

Therefore water plays a catalytic role in this multistep equilibrium, which can be explained as follows. The oligomerization process implies nucleophilic attack on a boron atom by the oxygen atom of another monomeric unit. The nucleophilicity of the oxygen atom of $\mathbf{1}_m$ is low, due to the intramolecular $p\pi-p\pi$ O→B electron donation.⁴ Water coordination on $\mathbf{1}_m$ destroys this interaction, making the nonbonding electrons of the OH group more available for intermolecular interaction with another boron center. Indeed, a comparison of the electrostatic potential maps for the monomer $\mathbf{1}_m$ and the water adduct **5** (Figure 11) clearly evidences an enhanced nucleophilicity of the oxygen atom in **5**.

This opens alternative pathways for the transformation of $\mathbf{1}_m$ into $\mathbf{1}_t$: the mechanism for this oligomerization process, both in the absence and in the presence of water, has been investigated by means of PM3 calculations. Scheme 2 reports the proposed steps and intermediates, together with relative energies computed at the B3LYP/6-31G(d,p)/PM3 level of theory. We must remark that computed energy values have to be considered with caution, due to the known limitations of PM3 in describing hydrogen-bond and transition structure geometries.²⁶ Moreover, reported energies do not take into account the entropic contribution, which is expected to be important for an association process, but difficult to estimate, particularly for solution phase reactions. However, the overall qualitative picture depicted by the above computations well agrees with the main experimental findings.

The absence of enthalpic barriers for the formations of the water adducts **5** and **4** is in line with the fast

(23) It is worthwhile to remark that the formation of the two water adducts did not occur in the rigorous stepwise manner observed for the adducts between $\text{B}(\text{C}_6\text{F}_5)_3$ and water.¹ Indeed, the shift of the ^{11}B signal was not complete during the first titration step (Figure 10d) and the change of the slope of the ^{19}F titration plots in correspondence with 1 equiv of water was less sharp than in the case of the analogous titration of $\text{B}(\text{C}_6\text{F}_5)_3$ with water.¹ Furthermore, the δ shift of the ^{19}F and ^{11}B signals did not stop exactly in correspondence with 2 equiv of water, indicating that an excess of water is necessary to completely drive to the right the association equilibria. At further variance with respect to what is observed for $\text{B}(\text{C}_6\text{F}_5)_3$, the water molecule in **5** was labile enough to allow very fast water exchange between $\mathbf{1}_m$ molecules, resulting in averaged resonances for $\mathbf{1}_m$ and its water adduct **5**. By contrast, $\text{B}(\text{C}_6\text{F}_5)_3$ and $(\text{C}_6\text{F}_5)_3\text{B}-\text{OH}_2$ gave separated signals at temperatures lower than 273 K.^{1,2a}

(24) The ^{19}F and ^1H δ values of $\mathbf{1}_m$ and $\mathbf{1}_t$ reported in Table 1 have been determined in the presence of $\text{B}(\text{C}_6\text{F}_5)_3$, as water scavenger.

(25) The progressive sharpening of the averaged resonances of $\mathbf{1}_m$ observed in the course of the titration monitored at 283 K (Figure 9) is likely attributable both to the increased water mobility and to the decreased $\Delta\delta$ between the exchanging sites (revealed by the decrease of the slopes of Figure 10), as previously observed for $\text{B}(\text{C}_6\text{F}_5)_3$.¹

(26) Jensen, F. *Introduction to Computational Chemistry*; Wiley: Chichester, U.K., 1999; Chapters 3 and 11.

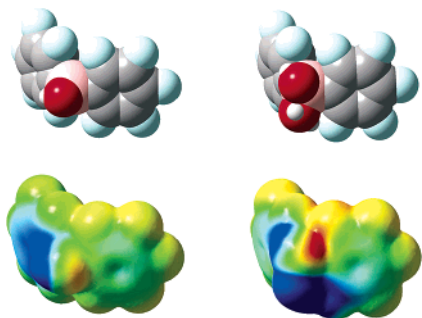


Figure 11. Space-filling models and electrostatic potential mapped onto the electron density isosurfaces (0.0004 au) for the monomer **1_m** and the water adduct **5** (B3LYP/6-31G(d,p)//PM3). Dark red (blue) corresponds to -0.03 ($+0.03$) au.

exchanges (leading to averaged NMR signals) observed between **1_m** or **1_t** and their respective adducts **5** and **4**.

The water adduct **5** bears both a reactive OH group (see Figure 11) and a coordinated water molecule prone to be involved as a donor in a hydrogen bond: the presence of these two reactive sites makes easier the association of monomeric units and leads at first to the formation of the dimeric intermediate **I1** of Scheme 2 and eventually to the trimer **3**.

The species **3** appears kinetically inert with respect to its transformation into the closed cyclic trimer **1_t** or **4**. Indeed its isomerization into **I2** is accompanied by a quite high energy barrier. This can be explained observing that the strong hydrogen bond present in **3** has been replaced in the intermediate **I2** by a weaker O–H...OH₂ interaction. The subsequent substitution reaction at the boron atom that leads to **4** shows a quite high energy barrier as well. Therefore **3** is not a good intermediate in the monomer to trimer pathway.

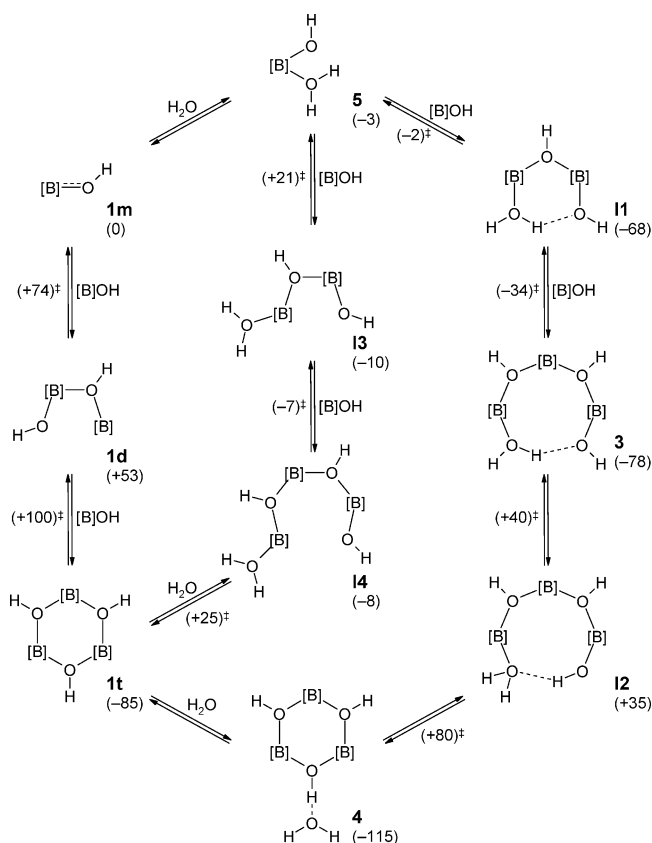
A better pathway for the **1_m** ⇌ **1_t** interconversion is provided by the formation of the oligomeric open species **I3** and **I4** depicted in the center of Scheme 2. In particular, in **I4** the water molecule and the OH group show the correct relative position to undergo a nucleophilic substitution: the energy barrier is much lower (by 75 kJ mol⁻¹) than computed in the absence of water (left part of Scheme 2) and fully accounts for the observed catalytic role of water. Attempts to find a direct interconversion pathway between the open **I4** and the hydrogen-bonded species **3** failed, because the opening requires rotation around the H₂OB–O(H)B bond, hampered by the presence of the two bulky pentafluorophenyl substituents on the boron atom.

The relative kinetic barriers and enthalpic stabilities of Scheme 2 also agree with the fact that **3** was the only detected species, among all the dimeric and trimeric water-containing intermediates of Scheme 2.

The experimental data clearly indicated that at low temperatures the **1_m** ⇌ **1_t** equilibrium became exceedingly slow. In other words, in these conditions the communications between closed trimers (**1_t** plus **4**) and monomers (**1_m** plus **5**) are blocked. The latter species, however, maintain their communication with **3** (and the easy exchange between **3** and **1_m**, revealed by the EXSY at 173 K, indicates that at least the step from **I1** to **3** must be fast).

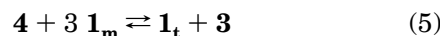
Finally, both the experimental data and computational results agree with the fact that **3** is formed (at

Scheme 2. Oligomerization Equilibrium in the Absence (left) and Presence (center and right) of Water^a



^a [B] refers to the (C₆F₅)₂B moiety. Relative energies (kJ mol⁻¹) computed at the B3LYP/6-31G(d,p)//PM3 level are given in parentheses.

very low temperatures only, for entropic reasons) from **1_m**, while its formation by cycle opening from **1_t** (or **4**) is strongly disfavored. Curiously, the formation of **3** is generally accompanied by a decrease of the concentration of **4**, but this results from water transfer and not from direct water insertion into the cycle. Indeed, at room temperature (or slightly lower) adventitious water necessary for the formation of **3** is bound to the trimer (giving **4**). So, on lowering the temperature below 230 K, we observe the progressive shift of the ¹⁹F and ¹H signals of the trimer (averaged signals **1_t** plus **4**) toward their “anhydrous” values (as shown in Figure S7 in the Supporting Information), due to the uptake of the released water by **3**. The formation of **3** from adventitious water is then better described by equilibrium 5 rather than equilibrium 3. On increasing back the temperature, the chemical shifts varied in the opposite way, indicating the reversal of this equilibrium.



Conclusions

The present investigation has shown that the trimeric form of the title compound is not peculiar to the solid state but can also be present in solution, the trimerization being favored in nonaromatic solvents of low polarity. A solvent of relatively high polarity like dichloromethane permits trimer concentrations sufficiently high to allow the study of the oligomerization equilibrium.

The ratio between monomeric and trimeric forms present in CD₂Cl₂ solution was found very variable, depending not only on thermodynamic (temperature, concentration) but also on kinetic factors (the elapsed time at a given temperature, and even the rate by which this temperature was reached). Indeed, the attainment of equilibrium is very slow, and this greatly hampers the determination of the equilibrium concentration at temperatures lower than room temperature. This is attributable to the intramolecular oxygen-to-boron π -donation, which reduces both the Lewis acidity of boron and the Lewis basicity of oxygen.

Moreover, the presence of water affects both the kinetics and the thermodynamics of this equilibrium. Water catalyzes the attainment of equilibrium due to the increased nucleophilicity of the oxygen atom upon water coordination. Semiempirical computations have fully confirmed this experimental finding, allowing us to depict a trimerization pathway with a lower kinetic barrier than under anhydrous conditions. The same computations have also confirmed the observed stabilization of the trimeric form in the presence of traces of water, due to the formation of a stable hydrogen-bonded adduct containing exocyclic water.

The preferential H-bond interaction of water with the trimer rather than with the monomer is attributable to the higher effective electronegativity of an oxygen atom bound to two acidic boron centers. On the other hand, the preferential formation of an H-bond interaction (with **1_t**) rather than a Lewis acid–base covalent bond (with **1_m**) confirms the low Lewis acidity of the boron atom in **1_m**.

The capability of modifying both the rate and the position of the oligomerization equilibrium should be a property that water shares with other Lewis bases. This will be the subject of future investigations.

Peculiar of water, on the contrary, is the capability of generating the trimeric adduct **3** containing a water molecule within an octaatomic O–B–O–B–O–B–O–H cycle, closed by a very strong hydrogen bond. The stabilization of the (simultaneously H-bonded and B-bonded) water molecule in **3** is strong enough to promote water formation, by dehydrating borinic acid to its anhydride. Low-temperature CH₂Cl₂ solutions of the title compound can therefore be considered water scavengers more powerful than the anhydride **2** itself.

Experimental Section

All manipulations were performed under N₂ or Ar using oven-dried Schlenk-type glassware. CD₂Cl₂ (C.I.L.) was anhydri-fied on activated molecular sieves. B(C₆F₅)₂OH was a gift from Basell Polyolefins.

All NMR spectra were acquired on a Bruker AVANCE DRX-300 spectrometer, equipped with a 5 mm TBI probe (90° pulse: ¹H 8.5 μ s, ¹⁹F 24 μ s, ¹¹B 9 μ s) or with a 5 mm QNP probe (90° pulse: ¹H 7.0 μ s, ¹⁹F 8.6 μ s) and on a Bruker AC300 spectrometer equipped with a 5 mm BBO probe (90° pulse: ¹H 7.2 μ s, ¹¹B 6.6 μ s). ¹⁹F NMR spectra were referenced to external CFC₃. The DOSY experiment and a low-temperature ¹H spectrum shown in Figure S4 have been recorded at 11.7 T on a Bruker AMX-500 WB spectrometer. The temperature was calibrated with a standard CH₃OH/CD₃OD solution.²⁷

Equilibration Experiments at Different Concentrations and Temperatures. A sample of **1** (23.8 mg, 0.066

mmol) was dissolved in CD₂Cl₂ (0.6 mL) in a NMR tube, and ¹⁹F NMR spectra were acquired at 283 K at different times until the **1_m**/**1_t** ratio remained constant. The sample was diluted by CD₂Cl₂ addition (0.32 mL), and the equilibration was then monitored at the same temperature. Then the temperature was lowered (at first at 273 K, and successively at 263 and 253 K), and at each temperature the equilibration was monitored, resulting in the data of Figure 3.

To study the effect of concentration, the equilibration process was monitored by ¹⁹F NMR at 278 K on another sample of **1** (initially 0.0771 M), treated with increasing amounts of **1**, affording solutions of 0.110, 0.140, 0.186, and 0.202 M (Figure 2).

Dynamics of 1_m. Variable-temperature ¹⁹F spectra were recorded on a 0.141 M sample of **1**. The kinetic constants for the restricted rotation around the B–O bond of **1_m** were obtained by band shape analysis, using the coupling constants J_{FF} , estimated from the simulation of a room-temperature spectrum with Bruker WINDAISY software ($J_{23} = -23.0$, $J_{24} = -4.2$, $J_{25} = 9.8$, $J_{26} = -4.8$, $J_{34} = -20.5$, $J_{35} = 0.2$ Hz): k , s⁻¹ (T , K): 24 (183), 90 (192), 280 (201), 1090 (211), 3400 (221). In the band shape analysis the contribution of the exchange between **1_m** and **3** was neglected, since the rate of the latter process, as estimated from 2D EXSY volumes, was about 1 order of magnitude smaller than that of the intramolecular process in **1_m**.

Addition of Water Scavengers to Two Solutions of 1. A 0.10 M solution of **1** in CD₂Cl₂ was treated in a NMR tube with a few molecular sieves. ¹H and ¹⁹F spectra were recorded at 278 K every 5 min for 3 h. The spectra (data not shown) revealed (i) a progressive slight upfield shift of the ¹H signal of the trimer (due to the slow conversion of **4** into **1_t**); (ii) the simultaneous decrease of the relative intensity of the signal of the trimer with respect to the monomer (due to the loss of the stabilization of the trimer upon hydrogen bonding with water); and (iii) the sharpening of the ¹H signal of **1_m** (the broadening being due to intermolecular proton exchange processes). No significant formation of anhydride was observed in this time. Then, solid B(C₆F₅)₃ (ca. 0.3 equiv) was added directly in the NMR tube and ¹H and ¹⁹F were recorded, showing (i) the formation of some B(C₆F₅)₃–OH₂ adduct; (ii) a slight further shift upfield of the protonic signal of **1_t**; and (iii) the formation of a significant amount (0.12 equiv) of anhydride **2**. In another experiment, different aliquots of P₄O₁₀ were added directly into a NMR tube containing a 0.069 M solution of **1** in CD₂Cl₂: each addition caused a sudden increase of the amount of the anhydride **2**, up to the conversion of ca. 65% of **1** into **2**, as revealed by the ¹H and ¹⁹F spectra at 270 K.

Titration with Water. A 0.18 M sample of **1** was prepared by dissolving 35.5 mg of **1** in 0.54 mL of CD₂Cl₂ in a NMR tube. Water additions (0.1–0.5 μ L, up to 3.5 equiv) were made at room temperature, and ¹H, ¹⁹F, and ¹¹B NMR spectra were recorded at 283 K after each addition (Figures 9 and 10). An analogous experiment (without ¹¹B monitoring) was performed at 253 K.

Computational Study. Geometry optimizations have been performed at the PM3 semiempirical level, employing SPARTAN 02.²⁸ No symmetry has been imposed; however **1_m** and **1_t** possess C_s and C_2 symmetry, respectively, and the overall structures of **1_t**, **3**, and **4** deviate only marginally from C_2 symmetry (in **1_t** and **3** this is due to the asymmetry of the hydrogen bond and in **4** to the position of the water molecule with respect to the pseudo- C_2 axis). Optimizations have been done employing the Hessian matrix computed at the PM3 level; the convergence criteria in geometry optimization for the maximum gradient component and the maximum change in a bond length have been set to 10⁻⁵ au and 10⁻⁴ Å. The nature (true minima or first-order transition structures) of all the stationary points found have been determined by computing

(27) Van Geet, A. L. *Anal. Chem.* **1970**, *42*, 679.

(28) SPARTAN 02; Wavefunction Inc.: Irvine, CA, 2002.

the Hessian matrix. Some of the transition states have been located driving some internal coordinates (mainly bond distances) corresponding to the expected reaction coordinates. Successively, the eigenvector associated with the negative eigenvalue has been followed in both directions (by minimizing two slightly distorted structures) to ascertain that the transition structure links the two expected minima. Single-point computations of the energies at the B3LYP/6-31G(d,p) level have been done with GAUSSIAN 98.²⁹

Acknowledgment. T.B. and G.D. thank Basell Polyolefins for partial funding of this work and for providing samples of the title compound. P.M. and A.S. acknowl-

edge Prof. Maurizio Sironi for the use of SPARTAN 02. Thanks are also due to Italian CNR (ISTM) for providing facilities for inert atmosphere and low-temperature experiments and to Mrs. M. Bonfà for the experiments at 11.7 T.

Supporting Information Available: Seven figures showing details of the NMR experiments. This material is available free of charge via the Internet at <http://pubs.acs.org>.

OM0494519

(29) *GAUSSIAN 98* (revision A.11.3); Gaussian Inc.: Pittsburgh, PA, 2002.